



# A GXXXA Motif in the Transmembrane Domain of the Ebola Virus Glycoprotein Is Required for Tetherin Antagonism

Mariana González-Hernández,<sup>a</sup> Markus Hoffmann,<sup>a</sup> Constantin Brinkmann,<sup>a</sup> Julia Nehls,<sup>b,c</sup> Michael Winkler,<sup>a</sup> Michael Schindler,<sup>b,c</sup>  Stefan Pöhlmann<sup>a</sup>

<sup>a</sup>Infection Biology Unit, German Primate Center, Göttingen, Germany

<sup>b</sup>Institute of Medical Virology and Epidemiology of Viral Diseases, University Hospital Tübingen, Tübingen, Germany

<sup>c</sup>Institute of Virology, Helmholtz Center Munich, German Research Center for Environmental Health, Neuherberg, Germany

**ABSTRACT** The interferon-induced antiviral host cell protein tetherin can inhibit the release of several enveloped viruses from infected cells. The Ebola virus (EBOV) glycoprotein (GP) antagonizes tetherin, but the domains and amino acids in GP that are required for tetherin antagonism have not been fully defined. A GXXXA motif within the transmembrane domain (TMD) of EBOV-GP was previously shown to be important for GP-mediated cellular detachment. Here, we investigated whether this motif also contributes to tetherin antagonism. Mutation of the GXXXA motif did not impact GP expression or particle incorporation and only modestly reduced EBOV-GP-driven entry. In contrast, the GXXXA motif was required for tetherin antagonism in transfected cells. Moreover, alteration of the GXXXA motif increased tetherin sensitivity of a replication-competent vesicular stomatitis virus (VSV) chimera encoding EBOV-GP. Although these results await confirmation with authentic EBOV, they indicate that a GXXXA motif in the TMD of EBOV-GP is important for tetherin antagonism. Moreover, they provide the first evidence that GP can antagonize tetherin in the context of an infectious EBOV surrogate.

**IMPORTANCE** The glycoprotein (GP) of Ebola virus (EBOV) inhibits the antiviral host cell protein tetherin and may promote viral spread in tetherin-positive cells. However, tetherin antagonism by GP has so far been demonstrated only with virus-like particles, and it is unknown whether GP can block tetherin in infected cells. Moreover, a mutation in GP that selectively abrogates tetherin antagonism is unknown. Here, we show that a GXXXA motif in the transmembrane domain of EBOV-GP, which was previously reported to be required for GP-mediated cell rounding, is also important for tetherin counteraction. Moreover, analysis of this mutation in the context of vesicular stomatitis virus chimeras encoding EBOV-GP revealed that GP-mediated tetherin counteraction is operative in infected cells. To our knowledge, these findings demonstrate for the first time that GP can antagonize tetherin in infected cells and provide a tool to study the impact of GP-dependent tetherin counteraction on EBOV spread.

**KEYWORDS** Ebola virus, glycoprotein, tetherin

The interferon (IFN) system is a component of innate immunity and constitutes the first line of defense against viral infection. The IFN response is characterized by three processes: the sensing of invading pathogens, the induction of signaling cascades, and the expression of IFN-stimulated genes (ISGs) (1–4). The entire spectrum of ISGs was first comprehensively characterized by Schoggins and colleagues (3), who showed that many of the 300 to 400 ISG-encoded proteins exert antiviral activity.

Received 8 March 2018 Accepted 13 April 2018

Accepted manuscript posted online 18 April 2018

**Citation** González-Hernández M, Hoffmann M, Brinkmann C, Nehls J, Winkler M, Schindler M, Pöhlmann S. 2018. A GXXXA motif in the transmembrane domain of the Ebola virus glycoprotein is required for tetherin antagonism. *J Virol* 92:e00403-18. <https://doi.org/10.1128/JVI.00403-18>.

**Editor** Terence S. Dermody, University of Pittsburgh School of Medicine

**Copyright** © 2018 American Society for Microbiology. All Rights Reserved.

Address correspondence to Stefan Pöhlmann, [spoehlmann@dpz.eu](mailto:spoehlmann@dpz.eu).

Understanding how ISG-encoded proteins inhibit viruses will provide not only important insights into how virus infection can be controlled by innate immunity but also a possible basis for novel antiviral strategies.

The host cell protein tetherin is upregulated by IFN (i.e., is encoded by an ISG) and is also constitutively expressed in certain cells and tissues (5, 6). Tetherin inhibits release of progeny particles from infected cells by forming a physical tether between the virus and host cell (6, 7). This activity critically depends on tetherin's particular domain organization: the protein harbors an N-terminal transmembrane domain (TMD) and a C-terminal glycosylphosphatidylinositol (GPI) anchor, which permit simultaneous insertion of tetherin into a viral and a cellular membrane. In response to the antiviral pressure imposed by tetherin, several viruses have evolved tetherin antagonists (8), including the HIV-1 protein Vpu (6), and most of these proteins block tetherin's antiviral activity by reducing tetherin levels at the site of viral budding, the plasma membrane (8).

The Ebola virus (EBOV), a member of the family *Filoviridae*, causes severe and frequently fatal disease in humans and nonhuman primates. The virus blocks signaling pathways of the IFN system via its VP24 and VP35 proteins (9). In addition, EBOV and other filoviruses counteract tetherin via their only virus-encoded surface protein, the viral glycoprotein (GP) (10–12). In this context, it should be noted that tetherin antagonism by GP has so far exclusively been demonstrated in cells releasing EBOV-like particles, and it is unknown if GP antagonizes tetherin in the context of EBOV infection and whether such antagonism is required for viral spread. In contrast to Vpu, EBOV-GP interferes with tetherin's antiviral activity without altering tetherin expression levels or cellular localization (12–14), and the mechanism underlying tetherin counteraction by EBOV-GP is largely unclear. Moreover, it is incompletely understood which domains in GP contribute to tetherin antagonism. Vande Burgt and colleagues reported a role for the glycan cap (15), and our previous work demonstrated that a single amino acid change in the receptor binding domain (RBD) can abrogate tetherin counteraction (10). In addition, the transmembrane domain (TMD) of EBOV-GP was shown to contribute to tetherin antagonism (15, 16), but the responsible amino acid motifs remain to be elucidated.

Here, we employed EBOV surrogate systems to investigate the contribution of a GXXXX motif in the TMD of EBOV-GP to tetherin antagonism. Although confirmation with infectious EBOV is pending and conclusions are thus tentative, our results indicate that the GXXXX motif, which was previously reported to be important for GP-mediated cell detachment (17), is also required for tetherin antagonism. Moreover, these results provide the first evidence that GP can antagonize tetherin in the context of infected cells.

## RESULTS

**Mutation of the GXXXX motif in the EBOV-GP TMD is compatible with robust GP expression and only modestly reduces GP-driven host cell entry.** To address the role of the GXXXX motif in the EBOV-GP TMD in tetherin antagonism, we first changed the GXXXX motif to LXXXXL using PCR-based mutagenesis (Fig. 1A). Next, we investigated GP expression and incorporation into viral particles, employing transiently transfected 293T cells. We found that EBOV-GP wild type (wt) and the LXXXXL mutant were expressed and proteolytically processed at comparable levels (Fig. 1B). Moreover, both wt GP and the LXXXXL mutant were comparably incorporated into vesicular stomatitis virus (VSV) pseudoparticles (Fig. 1C), which are frequently used to study EBOV-GP-driven entry, and the LXXXXL mutant mediated entry into cell lines derived from accidental hosts (humans and nonhuman primates) and a natural reservoir (fruit bat) with about half the efficiency of wt GP (Fig. 1D). Thus, the GXXXX motif is dispensable for GP expression and particle incorporation, and its mutation has only a modest effect on GP-driven host cell entry.

**The integrity of GXXXX motif is essential for tetherin antagonism.** Having demonstrated that the GXXXX motif is dispensable for GP expression and, to some

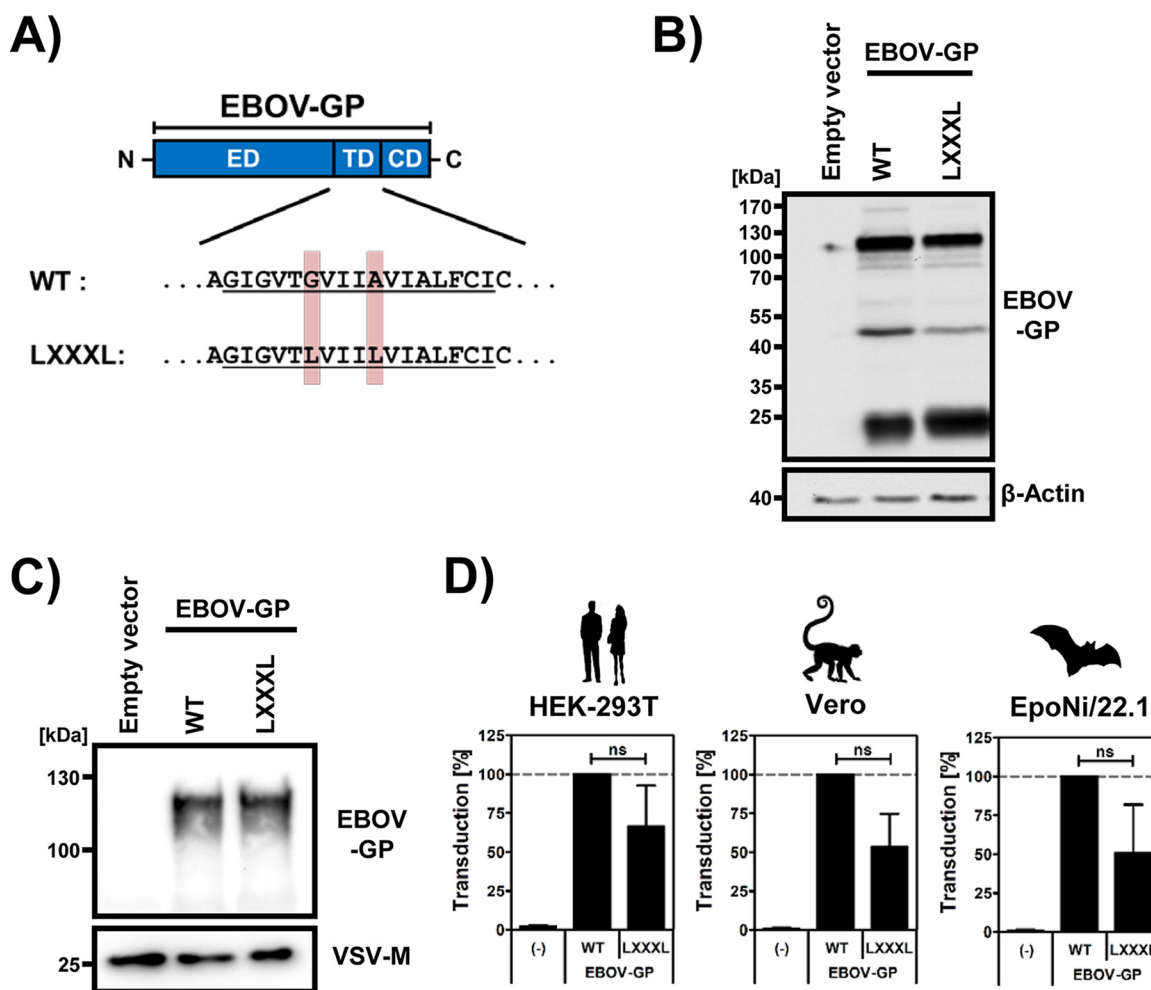


**FIG 1** Mutation of a GXXXA motif in the EBOV-GP TMD is dispensable for GP expression and particle incorporation but slightly reduces GP-driven host cell entry. (A) Sequence of the GXXXA motif in the EBOV-GP wt and LXXXL mutant (ED, ectodomain; TD, transmembrane domain [underlined]; CD, cytoplasmic domain). (B) Plasmids encoding V5-tagged versions of the indicated glycoproteins or empty plasmid (pCAGGS) as a negative control were transiently transfected into 293T cells. Expression of the GPs in cell lysates was detected using anti-V5 tag antibody. Detection of  $\beta$ -actin expression served as a loading control. Similar results were obtained in three independent experiments. (C) VSV pseudotypes harboring the indicated glycoproteins were concentrated from cell culture supernatants by centrifugation through a 20% sucrose cushion and then analyzed for the presence of EBOV-GP and VSV-M by Western blotting. The results were confirmed in three independent experiments. (D) The indicated human, nonhuman primate, and fruit bat cell lines were transduced with equal volumes of vesicular stomatitis virus (VSV) particles pseudotyped with the indicated GPs or with particles bearing no glycoprotein as negative controls. Luciferase activity in cell lysates, which was used as an indicator of transduction efficiency, was measured at 24 h posttransduction. Shown are normalized data from four experiments performed with independent pseudotype preparations, in which transduction mediated by EBOV-GP wt was set as 100%. Error bars indicate standard errors of the means, and statistical significance was analyzed using paired two-tailed *t* tests (ns, not significant).

extent, for GP-driven host cell entry, we next investigated if the GXXXA motif is required for tetherin antagonism. For this endeavor, we first employed a previously documented virus-like particle (VLP) assay, in which release of VLPs is driven by the HIV-1 p55 Gag protein and is inhibited by tetherin (12). In the Gag-based assay, VLPs were readily released from tetherin-negative control cells, and release was markedly reduced upon expression of tetherin (Fig. 2A and B). The tetherin-mediated restriction of VLP release was rescued upon coexpression of HIV-1 Vpu and EBOV-GP wt (Fig. 2A and B), as expected. In contrast, the LXXXL mutant was largely unable to promote VLP release from tetherin-positive cells (Fig. 2A and B), and this defect could not be rescued by expressing large amounts of the mutant (data not shown). Thus, the GXXXA motif is essential for efficient tetherin counteraction, at least under the conditions studied.

We next studied whether the LXXXL motif is also required for rescue of the release of EBOV-like particles from blockade by tetherin. For this, the above-described VLP

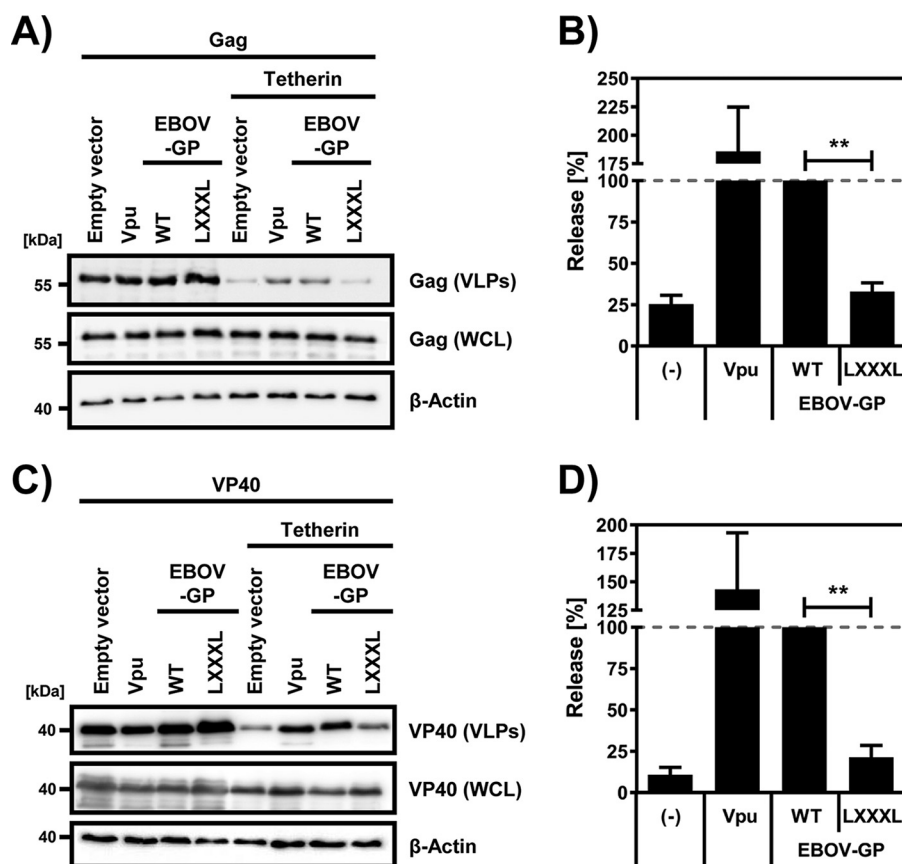


**FIG 2** The GXXXA motif is required for tetherin antagonism. (A) 293T cells were cotransfected with plasmids encoding HIV-Gag, the indicated glycoproteins or Vpu, and tetherin or empty plasmid. Cells and supernatants were harvested at 48 h posttransfection. Virus-like particles (VLPs) were pelleted by centrifugation through a 20% sucrose cushion. Whole-cell lysates (WCL) and VLPs were analyzed for the presence of Gag by Western blotting. Detection of  $\beta$ -actin expression served as a loading control. The results of a representative experiment are shown. (B) Three independent experiments conducted as described for panel A were quantified using the ImageJ program. VLP release from cells coexpressing EBOV-GP wt and tetherin was set as 100%. Error bars indicate standard errors of the means, and statistical significance was analyzed using a paired two-tailed *t* test (\*\*,  $P \leq 0.01$ ). (C) VLP release was examined as described for panel A, but EBOV-VP40 instead of HIV-Gag was used for particle production. (D) Four independent experiments conducted as described for panel C were quantified using the ImageJ program. VLP release from cells coexpressing EBOV-GP wt and tetherin was set as 100%. Error bars indicate standard errors of the means, and a paired two-tailed *t* test was used to determine statistical significance (\*\*,  $P \leq 0.01$ ).

assay was repeated using EBOV VP40 instead of HIV Gag. Expression of VP40 is sufficient for release of filamentous particles from cells (18, 19) and thus mimics release of EBOV from infected cells. In this assay, expression of EBOV-GP wt modestly increased the release of VLPs from tetherin-negative control cells (2-fold increase on average;  $n = 4$ ), in keeping with previous studies (20, 21), and rescued particle release from blockade by tetherin (Fig. 2C and D). Notably, the LXXXL mutant also promoted VLP release from tetherin-negative cells (1.5-fold increase on average;  $n = 4$ ) but failed to rescue particle release from blockade by tetherin (Fig. 2C and D). These results show that the GXXXA motif is also required for tetherin antagonism in the context of EBOV-like particles and that GP-mediated augmentation of particle release and GP-driven tetherin antagonism are genetically separable processes.

**The requirement of the GXXXA motif for tetherin antagonism is independent of membrane cholesterol levels.** The directed expression of GP in cells can induce cellular detachment (22, 23). A recent study reported that the mutation of the GXXXA motif to LXXXL or depletion of cholesterol reduces GP-driven cell detachment (17). We confirmed that mutation of GXXXA to LXXXL reduces cell detachment (Fig. 3A) and asked whether addition of cholesterol confers efficient tetherin antagonism to the

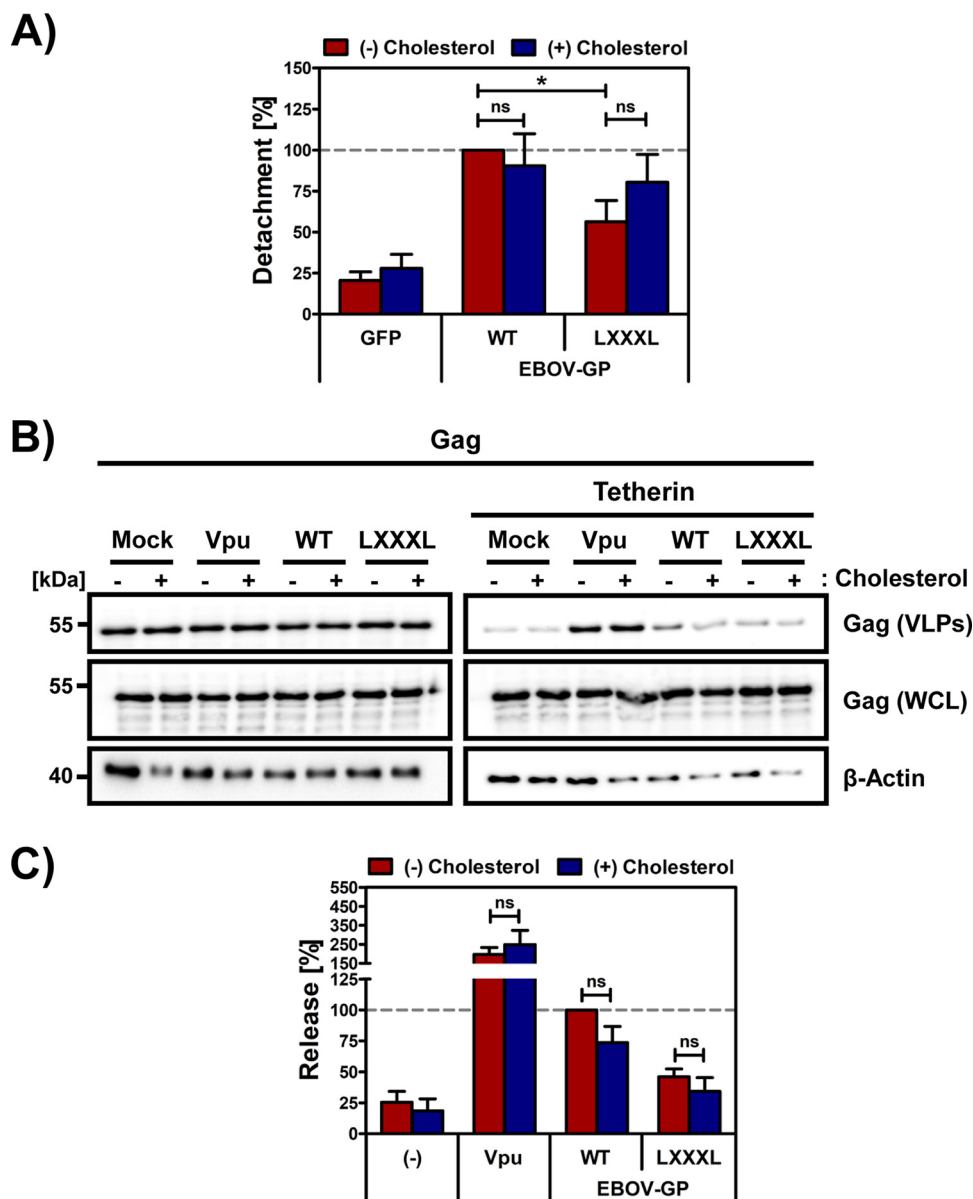


**FIG 3** Defective tetherin antagonism by mutant LXXXL cannot be restored with cholesterol. (A) HeLa cells were transiently transfected with plasmids encoding the indicated glycoproteins or GFP as a negative control. At 6 h posttransfection, cells were treated with water-soluble cholesterol at a concentration of 100  $\mu$ M or water alone for 30 min. Subsequently, cells were washed with PBS, and fresh medium was added. Supernatants were collected at 48 h after transfection, and the number of detached cells was quantified using flow cytometry. Shown are normalized data from five independent experiments carried out with triplicates samples, for which detachment driven by EBOV-GP wt was set as 100%. Error bars indicate standard errors of the means, and statistical significance was analyzed using one-way ANOVA with Bonferroni posttest analysis. (B) The HIV-Gag release assay was performed as described in the legend of Fig. 2; but at 6 h posttransfection water-soluble cholesterol was added at a final concentration of 100  $\mu$ M as indicated, and cells were incubated for 30 min. Afterwards, the cells were washed and incubated overnight. The results of a single representative experiment are shown. (C) Three independent experiments conducted as described for panel B were quantified using the ImageJ program. VLP release from cells coexpressing EBOV-GP wt and tetherin, but not treated with cholesterol, was set as 100%. For panels A and C, error bars indicate standard errors of the means, and statistical significance was analyzed using paired t test (ns, not significant; \*,  $P \leq 0.05$ ).

LXXXL mutant. However, cholesterol did not endow the LXXXL mutant with efficient tetherin antagonism and even reduced tetherin counteraction by wt GP (Fig. 3B and C), although not to a statistically significant degree. Thus, the GXXXA motif in the TMD of EBOV-GP is essential for efficient tetherin antagonism, and the requirement for this motif for tetherin counteraction is independent of membrane cholesterol.

### The GXXXA motif is required for robust viral spread in tetherin-positive cells.

Most previous analyses of tetherin counteraction by EBOV-GP were conducted with GP-transfected cells while infected cells were rarely studied. EBOV is a biosafety level 4 (BSL4) organism and could not be analyzed in the present study. However, VSV chimeras encoding EBOV-GP (VSV-EBOV-GP) afforded an opportunity to study EBOV-GP in the context of infected cells without the necessity of BSL4 conditions (24, 25). In order to analyze whether the GXXXA motif contributes to VSV-EBOV-GP spread in tetherin-positive cells, we generated VSV-EBOV-GP wt and VSV-EBOV-GP LXXXL via reverse genetics (Fig. 4A) and ensured by sequence analysis that the viruses had not acquired changes in GP during amplification in cell culture. Analysis of viral particles confirmed that the GP wt and LXXXL mutant were comparably incorporated into particles (Fig. 4B), as expected (Fig. 1C). Moreover, investigation of GP expression in infected cells showed that both wt and mutant GPs were expressed at similar levels (Fig. 4C). In order to analyze tetherin sensitivity of viruses bearing GP wt and mutant LXXXL, we infected Vero cells, which were stably transfected with empty vector (pQCXIP, control) or a tetherin-encoding vector and expressed high levels of tetherin (Fig. 4D). VSV wt was included as a control since this virus is highly tetherin sensitive (26, 27), and so far no VSV protein has been identified that antagonizes tetherin in infected cells. Infection of the Vero control cells (pQCXIP) revealed that VSV replicated more efficiently than VSV bearing EBOV-GP (Fig. 4E), as expected (24). Replication of VSV-EBOV-GP wt and mutant LXXXL was also readily detectable; but peak viral titers observed upon infection with the LXXXL mutant were about 10-fold reduced, and replication kinetics were delayed compared to the kinetics of infection with VSV-EBOV-GP wt virus (Fig. 4E). The expression of tetherin in target cells had a stronger inhibitory effect on peak viral titers (Fig. 4F) of VSV than of VSV-EBOV-GP, suggesting that GP-mediated tetherin antagonism might be operative in infected cells. More importantly, tetherin expression had a clearly more profound inhibitory effect on spread of the VSV-EBOV-GP LXXXL mutant than the VSV-EBOV-GP wt virus (Fig. 4E and F), indicating that the GXXXA motif was required for tetherin counteraction in VSV-EBOV-GP-infected cells.

## DISCUSSION

It remains largely enigmatic how EBOV-GP counteracts tetherin. Recent studies sought to obtain insights via mutagenic analyses. They showed that the glycan cap, the RBD, and the TMD contribute to tetherin antagonism (10, 15, 16). The observation regarding the TMD, jointly with the finding that a GXXXA motif within the EBOV-GP transmembrane domain is required for GP-mediated cellular detachment (17), prompted us to investigate whether the GXXXA motif contributes to tetherin antagonism. We show that the motif is dispensable for GP expression and particle incorporation but is required for efficient GP-driven tetherin antagonism. Our results underline an important contribution of the TMD to tetherin counteraction and provide, for the first time, evidence that GP can inhibit tetherin when expressed in the context of cells infected with an EBOV surrogate.

Our previous work provided the first hints toward a role of the EBOV-GP TMD in tetherin counteraction. We showed that the GP2 subunit of GP interacts with tetherin (12) and that replacing the EBOV-GP TMD with that of the Lassa virus glycoprotein (LASV-GPC, which does not antagonize tetherin) abrogates tetherin antagonism (16). However, only limited conclusions could be drawn from these results since EBOV-GP harboring the LASV-GPC TMD was unable to mediate entry (16). Moreover, LASV-GPC equipped with the EBOV-GP TMD failed to counteract tetherin (16). Strong evidence for a role of the EBOV-GP TMD in tetherin counteraction was then provided by Vande Burgt and colleagues. They showed that soluble GP (sGP), which is the primary translation product of the GP open reading frame (ORF), fails to counteract tetherin and that addition of the EBOV-GP TMD to sGP is sufficient to bestow tetherin antagonism upon sGP (15). However, the TMD amino acids required for tetherin antagonism remained unknown.

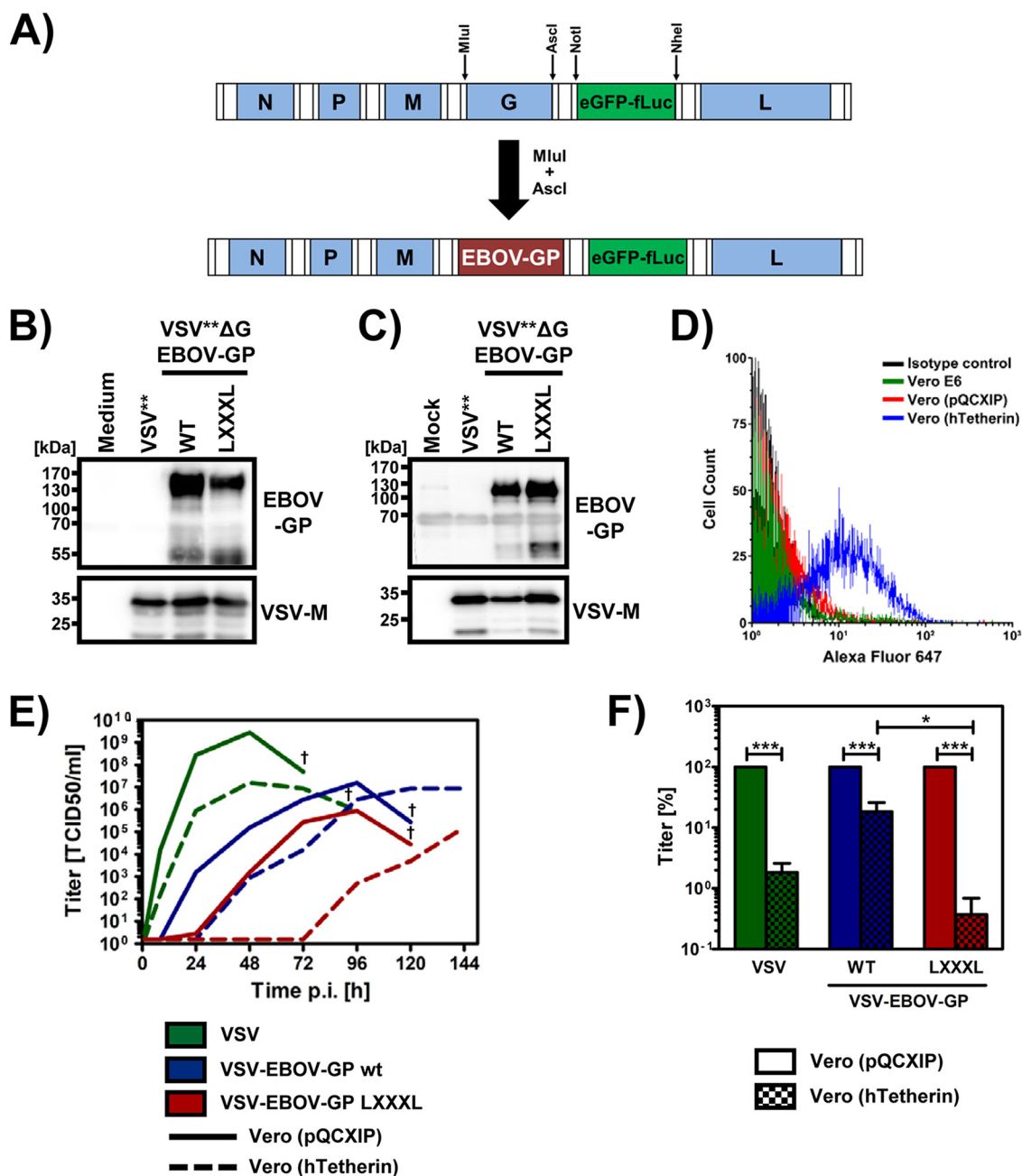


**FIG 4** Disruption of the GXXXA motif reduces EBOV-GP-dependent viral spread in tetherin-positive cells. (A) Schematic illustration of the VSV\*\* genome and the derived chimeric genome harboring the open reading frame (ORF) for EBOV-GP (red) instead of VSV-G. Transcription units coding for structural proteins of VSV are highlighted in light blue, while nontranslated regions of the genome are displayed in white. All VSV genomes code for a dual reporter consisting of eGFP linked to firefly luciferase from an additional transcription unit downstream of the respective glycoprotein ORF (green). (B) Replication-competent VSV chimeras encoding the indicated glycoproteins instead of VSV-G were pelleted through a 20% sucrose cushion and evaluated for incorporation of EBOV-GP and VSV-M by Western blotting. Similar results were obtained in two independent experiments. (C) Vero E6 cells were infected with VSV wt or the indicated VSV chimeras at an MOI of 1. At 20 h postinfection, cell lysates were prepared and analyzed for the expression of EBOV-GP (wt and mutant LXXXL) and VSV-M by Western blotting. Mock-infected and VSV wt-infected cells served as controls. Similar results were obtained in two independent experiments. (D) Tethrin surface expression on Vero cell lines used for the experiment shown in panel E was analyzed by flow cytometry. Vero (pQCXIP) were incubated with an isotype control and secondary antibody (black) or Vero E6 (green), Vero (pQCXIP) (red), Vero (hTetherin) (blue) cells were incubated with anti-tetherin antibody and secondary antibody. Antibody staining was analyzed by flow cytometry. A single representative experiment is shown; similar results were obtained in a second independent experiment. (E) Control Vero cells transduced with plasmid pQCXIP and Vero cells transduced to express human tetherin (hTetherin) were infected with VSV wt (green) or a VSV chimera coding for either EBOV-GP wt or the LXXXL mutant (MOI of 0.0001) for 1 h. After removal of the inoculum and washing of the cells, samples of the cell culture supernatants were taken at different time points (1, 8, 24, 48, 72, 96, 120, and 144 h postinfection), and viral titers were quantified by TCID<sub>50</sub> assay. The results of a single representative experiment are shown. Similar results were obtained in two additional, independent experiments.

(Continued on next page)

Our results show that a GXXXA motif within the TMD of EBOV-GP is essential for tetherin counteraction. The underlying mechanism is at present unclear. However, inferences can be made based on the work by Hacke and colleagues. They showed that the well-known ability of EBOV-GP to mediate the detachment of cells from a culture flask depends on the integrity of a GXXXA motif within the TMD and on the availability of membrane cholesterol (17). On the basis of these findings, they postulated that the GXXXA motif is required for interactions between GP trimers in cholesterol-rich microdomains (lipid rafts), which in turn is a prerequisite for GP-mediated detachment of cells and viral budding. Our results confirm that alteration of the GXXXA motif reduces cellular detachment and suggest that this defect can be rescued by cholesterol. However, addition of cholesterol to cells expressing the LXXXL mutant did not restore tetherin antagonism, and a previous report suggested that GP is neither located in lipid rafts nor alters tetherin localization in such domains (14). Moreover, evidence was provided that targeting sGP to lipid rafts is not sufficient for tetherin antagonism (15). In the light of these findings, membrane cholesterol does not seem to play a major role in tetherin antagonism by GP, and alternative scenarios should be considered. For instance, the GXXXA motif might contribute to formation and/or stability of GP trimers, and reduced trimerization might be incompatible with tetherin antagonism. However, our initial analyses revealed that particles bearing EBOV-GP wt and mutant LXXXL were comparably sensitive to inactivation by elevated temperature (data not shown), suggesting that the stability of the respective GP trimers may not be markedly different. Alternatively, the GXXXA motif might promote protein-protein interactions essential for tetherin antagonism. Given that the sequence integrity of the tetherin TMD is dispensable for GP-mediated tetherin antagonism (13), one can speculate that the GXXXA motif might mediate interactions of GP with a cellular protein that is required for tetherin counteraction.

Most studies employed VLP systems to analyze tetherin counteraction by EBOV-GP. In contrast, it remains unknown whether GP counteracts tetherin in the context of EBOV infection. Two studies provided evidence that EBOV infection might not be appreciably inhibited by tetherin (12, 28), but whether lack of tetherin sensitivity was due to the action of GP was not addressed. In the present study, alteration of the GXXXA motif in the context of VSV-EBOV-GP did not impact particle incorporation of GP and GP expression levels in infected cells. Moreover, mutation of the GXXXA motif only modestly reduced replication kinetics and peak viral loads in tetherin-negative cells, in keeping with the modestly diminished viral entry observed for the LXXXL mutant in single-cycle assays. In contrast, replication kinetics of the LXXXL mutant in tetherin-positive cells were markedly delayed compared to the kinetics of control cells while a clearly less pronounced delay was observed for the virus bearing wt GP. These results, jointly with the observation that VSV (which does not encode a tetherin antagonist that is active in infected cells) is more robustly inhibited by tetherin than VSV-EBOV-GP, suggest that tetherin counteraction by GP can occur in infected cells. Altering the GXXXA motif in the context of authentic EBOV might thus allow determination of the impact of GP-mediated tetherin antagonism on viral spread.

Based on these collective observations, we identified a mutation that abrogates tetherin antagonism with reasonable selectivity and consider it possible that even higher selectivity might be attainable by mutating only the glycine or the alanine residue within the GXXXA motif. Moreover, we provide, for the first time, evidence that GP can counteract tetherin in the context of cells infected with an EBOV surrogate. Future studies are required to confirm our results with infectious EBOV and to further elucidate how the GXXXA motif contributes to tetherin counteraction.

#### FIG 4 Legend (Continued)

Crosses indicate time points at which kinetics were stopped due to complete virus-induced cell lysis. (F) Mean viral peak titers (VSV wt, 48 h; VSV-EBOV chimeras, 96 h postinfection) resulting from inoculation of Vero control (pQCXIP) cells and Vero cells expressing hTetherin measured in three independent experiments conducted as described for panel E. Error bars indicate standard errors of the means, and statistical significance was analyzed using one-way ANOVA with Bonferroni posttest analysis (\*,  $P \leq 0.05$ ; \*\*\*,  $P \leq 0.001$ ).

## MATERIALS AND METHODS

**Cell culture.** HEK-293T (human, kidney), HeLa (human, cervix carcinoma), Vero and their subcloned derivative Vero E6 (both African green monkey, kidney), BHK-21(G43) (hamster, kidney), and EpoNi/22.1 (Buettikofer's epauletted fruit bat, kidney) cell lines were used as targets for transfection, transduction, infection, and detachment experiments. HEK-293T and HeLa cells (29) were obtained from DSMZ (ACC-635; Leibniz Institute DSMZ-German Collection of Microorganisms and Cell Cultures) and the NIH AIDS reagent program (<https://www.aidsreagent.org/>), respectively, while Vero, Vero E6, BHK-21(G43) (30), and EpoNi/22.1 (12) cells were provided by collaborators. All cell lines were maintained in Dulbecco's modified Eagle medium (PAN-Biotech), supplemented with 10% fetal bovine serum (Biocrom) and 1% penicillin-streptomycin (PAN-Biotech). Medium for EpoNi/22.1 cells was additionally supplemented with 1 mM sodium pyruvate (PAA Laboratories) and 1× nonessential amino acids (from a 100× stock solution; PAN-Biotech). After being transfected with the retroviral pQCXIP vector, Vero cells stably expressing human tetherin [Vero (hTetherin)] and Vero control cells expressing pQCXIP [Vero (pQCXIP)] were selected and maintained using 10 and 0.5 μg/ml of puromycin (Cayman chemical), respectively. All cells were incubated in a humidified atmosphere at 37°C and 5% CO<sub>2</sub>. For subcultivation and seeding, cells were detached by either resuspension in fresh culture medium (HEK-293T cells) or by the use of trypsin-EDTA (PAN-Biotech).

**Plasmids.** Expression plasmids encoding the proteins used in this study were described previously, as follows: EBOV and VSV glycoproteins EBOV-GP (GenBank accession number [AF086833.2](#)) and VSV-G, respectively (10, 31); human tetherin (32); HIV-1 Vpu (12); HIV-1 p55-Gag (12, 16); and EBOV-VP40 harboring an N-terminal c-Myc epitope, EQKLISEEDL (33). The GXXXA motif in the transmembrane of EBOV-GP was genetically modified to LXXXL by employing overlap extension PCR. Expression plasmids for the coding sequences of VSV nucleoprotein (VSV-N), phosphoprotein (VSV-P), and RNA-dependent RNA-polymerase (VSV-L) were generated by amplifying the respective open reading frames (ORF) from a plasmid-encoded VSV anti-genome (Indiana strain; kindly provided by G. Zimmer) and inserting them via standard cloning procedures into the pCAGGS expression vector.

In order to produce replication-competent, chimeric VSV expressing EBOV-GP wild-type (wt) or the LXXXL mutant instead of VSV-G, as well as a dual reporter consisting of an enhanced green fluorescent protein (eGFP) and firefly luciferase (fLuc) from an additional transcription unit, we generated a plasmid-encoded VSV anti-genome (GenBank accession number [J02428.1](#)) as follows. First, we introduced unique MluI and NheI restriction sites upstream and downstream of the VSV-G transcription unit, respectively. Next, a cassette was inserted that consisted of the coding sequences of VSV-G and the eGFP-fLuc dual reporter, separated by a minimal intergenic region (34). To obtain the eGFP-fLuc dual reporter, the stop codon of the eGFP open reading frame (ORF) was removed and then combined with the genetic information of fLuc, linked via a nonflexible amino acid linker sequence (GPDPPVAT). This strategy gave rise to VSV\*\* (the two asterisks indicate the dual reporter, later referred to as VSV). As this construct also contained a unique AscI restriction site downstream of the VSV-G transcription unit, it allowed us to replace VSV-G with the EBOV-GP wt or mutant LXXXL, thus generating VSV\*\*ΔG EBOV-GP wt, VSV-EBOV wt, VSV\*\*ΔG EBOV-GP LXXXL, and VSV-EBOV LXXXL. The integrity of all PCR-amplified sequences was verified by automated sequence analysis.

**Detachment assay.** HeLa cells were transiently transfected following calcium-phosphate precipitation with plasmids encoding EBOV-GP wt, EBOV-GP LXXXL, or GFP as a control. At 6 h posttransfection, cells were treated with water-soluble cholesterol (Sigma) at a concentration of 100 μM or water alone for 30 min. Subsequently, cells were washed with phosphate-buffered saline (PBS), and fresh medium was added. Supernatants were collected at 48 h after transfection, and the number of detached cells was quantified using a Becton Dickinson LSR II flow cytometer and BD FACSDIVA software.

**Production of rhabdoviral pseudotypes.** The pseudotypes were generated and used for transduction as described previously (35). In brief, 293T cells were seeded in six-well plates and transfected by calcium phosphate precipitation with plasmids encoding VSV-G, EBOV-GP wt, or EBOV-GP LXXXL or with an empty plasmid (pCAGGS) as a negative control. At 18 h posttransfection, the cells were inoculated with a replication-deficient VSV, in which the ORF for VSV-G was replaced by two separate ORFs for eGFP and fLuc (36) (kindly provided by G. Zimmer), at a multiplicity of infection (MOI) of 3. At 1 h postinfection, cells were washed with PBS and incubated with a 1:1,000 dilution of I1 (an anti-VSV-G mouse hybridoma supernatant from CRL-2700; American Type Culture Collection) for 1 h at 37°C in order to neutralize residual input virus. Finally, fresh culture medium was added to the cells. At 18 to 20 h posttransduction, supernatants were collected, clarified from cell debris by centrifugation, aliquoted, and stored at –80°C until use.

**Transduction of cell lines and quantification of fLuc activity.** To assess cell entry driven by EBOV-GP LXXXL, 293T, Vero E6, and EpoNi/22.1 cells were seeded in 96-well plates. At 24 h after seeding, medium was removed, and cells were transduced with equal volumes of VSV pseudotypes. At 16 to 18 h posttransduction, intracellular fLuc activity was measured as an indicator of transduction efficiency. For this, the cell culture medium was aspirated, and cells were incubated for 30 min at room temperature with 50 μl of luciferase cell culture lysis reagent (Promega). Lysates were transferred to a white, opaque-walled 96-well plate (Thermo Scientific), and fLuc activity was measured in a microplate reader (Plate Chameleon; Hidex) using MicroWin2000 software (version 4.44; Mikrotek Laborsysteme, GmbH) and fLuc substrate from a Beetle-Juice kit (PJK GmbH).

**Rescue and quantification of replication-competent VSV chimeras encoding EBOV-GP wt and EBOV-GP LXXXL.** For the rescue of the replication-competent VSV-EBOV wt or LXXXL, we used a strategy developed by others (37) with some modifications. First, BHK-21(G43) cells were seeded in 12-well plates and treated with mifepristone (Sigma-Aldrich) at a final concentration of 1 nM [BHK-21(G43) cells

inducibly express VSV-G upon stimulation with mifepristone] (30). At 16 h posttreatment, cells were infected with recombinant modified vaccinia virus Ankara expressing T7 polymerase (vMVA-T7; kindly provided by G. Sutter) (38) at an MOI of 3. The inoculum was aspirated 1 h after infection, and cells were washed with PBS. Next, the cells were transfected with expression plasmids for VSV-N, -P, and -L (polymerase complex) as well as the respective plasmid-encoded VSV anti-genome using Lipofectamine 2000 (ThermoFisher Scientific) as a transfection reagent. In this anti-genome, a T7 promoter sequence that precedes the leader region of the VSV genome drives cytoplasmic synthesis for negative-sense, full-length VSV genomes with defined genome ends through the activity of the hepatitis delta virus ribozyme located directly downstream of the trailer region. The negative-sense, full-length VSV genomes serve then as templates for mRNA transcription and further genome replication (both driven by the VSV polymerase complex). The following DNA amounts per well were used: 0.4  $\mu\text{g}$  of VSV-N, 0.35  $\mu\text{g}$  of VSV-P, 0.25  $\mu\text{g}$  of VSV-L, and 1  $\mu\text{g}$  of plasmid-encoded VSV anti-genome. At 6 h posttransfection, cells were washed, and fresh medium containing 1 nM mifepristone was added. We used mifepristone-stimulated BHK-21(G43) cells for initial transcomplementation of newly produced VSV particles with VSV-G in order to boost rescue efficiency. At 18 h posttransfection, the culture medium was supplemented with 100  $\mu\text{g}/\text{ml}$  rifampin and 40  $\mu\text{g}/\text{ml}$  cytosine  $\beta$ -D-arabino-furanoside (both from Sigma-Aldrich) to limit rMVA-T7 replication. After an additional 48 h of incubation, the supernatant was collected, clarified from cellular debris by centrifugation (4,700 rpm, 10 min, 4°C), and twice filtered through 0.2- $\mu\text{m}$ -pore-size filter membranes to exclude residual rMVA-T7 from the preparation. Next, Vero E6 cells grown in a T-25 flask were inoculated with a 1:3 dilution of the filtered supernatant and incubated for 72 h in the presence of anti-VSV-G mouse hybridoma supernatant to neutralize subsequent host cell entry by *in trans*-delivered VSV-G. Afterwards, culture medium was collected and filtered again. Finally, Vero E6 cells grown in a T-75 flask were inoculated with a 1:10 dilution of the supernatant for virus stock production.

Quantification of titers of virus stocks was carried out on confluent Vero E6 cells seeded in 96-well plates. First, cell culture medium was removed, and cells were inoculated with 10-fold serial dilutions of virus. At 1 h postinfection, inoculum was removed, and cell culture medium containing 2% methylcellulose (Sigma-Aldrich) was added. After 48 h of incubation, eGFP-positive foci were counted under a fluorescence microscope. Virus stock titers were determined as the number of focus forming units (FFU) per milliliter to calculate the MOI for subsequent infection experiments. To verify the integrity of VSV-EBOV wt and VSV-EBOV LXXXL, viral RNA was extracted from virus stocks using a QIAamp Viral RNA minikit (Qiagen) and reverse transcribed into cDNA using a SuperScript III first-strand synthesis system (ThermoFisher Scientific) according to the manufacturer's protocol (for random hexamers). A fragment of approximately 1,800 bp was then amplified with primers binding in the intergenic region upstream of EBOV-GP (forward) and near the 5' end of the eGFP ORF (reverse) using Phusion polymerase (ThermoFisher Scientific), separated by agarose gel electrophoresis, and extracted from the gel by commercial kits (Macherey & Nagel), before being subjected to automated sequence analysis (SeqLab).

**Growth kinetics of VSV-EBOV-GP in control and tetherin-positive cells.** To evaluate the effect of the GXXXA motif on viral spread, Vero cells stably expressing human tetherin (hTetherin) or control Vero cells containing empty vector (pQCXIP) were infected with VSV-EBOV-GP wt or VSV-EBOV-GP LXXXL (MOI of 0.0001) for 1 h. Afterwards, cells were washed with PBS to remove residual inoculum, and fresh culture medium was added. Cells were further incubated, and samples were collected at 1, 8, 24, 48, 72, 96, 120, and 144 h postinfection. Viral titers were determined on Vero E6 cells by calculating the 50% tissue culture infective dose ( $\text{TCID}_{50}$ ) according to the Spearman-Kärber method (39, 40).

**Analysis of tetherin surface expression by flow cytometry.** For analysis of tetherin surface expression, Vero E6, Vero control (pQCXIP), and Vero cells stably expressing human tetherin were detached and incubated for 30 min at 4°C with a 1:50 dilution of purified anti-human CD317 (BST2; tetherin) antibody (BioLegend) or with an isotype-matched control antibody (BioLegend). Afterwards, cells were washed twice with PBS and then incubated with Alexa Fluor 647-conjugated goat anti-mouse secondary antibody at a 1:100 dilution for 30 min at 4°C. Finally, cells were washed with PBS, fixed with 2% paraformaldehyde (PFA), and analyzed in a Becton Dickinson LSR II flow cytometer. Data were further analyzed using FCS Express, version 4, software.

**Immunoblotting.** Expression and incorporation of EBOV-GP wt and EBOV-GP LXXXL into VSV pseudotypes and replication-competent VSV-chimeras were determined by Western blotting. For expression analysis, HEK-293T cells were transiently transfected with plasmids encoding EBOV-GP wt, EBOV-GP LXXXL (both harboring an N-terminal V5 tag), or empty plasmid (pCAGGS) as a negative control. At 48 h posttransfection, culture medium was aspirated, and cells were lysed using 300  $\mu\text{l}$  of 2 $\times$  sodium dodecyl sulfate (SDS)-containing lysis buffer (50 mM Tris [pH 6.8], 10% glycerol, 2% SDS, 5%  $\beta$ -mercaptoethanol, 0.1% bromophenol blue, 1 mM EDTA) and boiled for 30 min at 95°C. To assess EBOV-GP wt and EBOV-GP LXXXL incorporation into pseudotypes and VSV-EBOV chimeras, equal volumes of pseudotype preparations or supernatant of virus stocks were pelleted by centrifugation (17,000  $\times g$ , 2 h, 4°C) through a 20% sucrose cushion. Samples were resuspended in 20  $\mu\text{l}$  of 2 $\times$  SDS lysis buffer and boiled for 30 min at 95°C. Afterwards, samples were separated by SDS-PAGE using 12.5% polyacrylamide gels and transferred onto nitrocellulose membranes (0.2- $\mu\text{m}$  pore size; GE Healthcare Life Sciences). Membranes were blocked for 1 h in 5% milk powder in PBS with 0.1% Tween 20. The expression of V5-tagged glycoproteins was detected using anti-V5 antibody (Invitrogen) at a 1:1,000 dilution;  $\beta$ -actin was detected after the membranes were stripped (Tris-HCl, SDS,  $\beta$ -mercaptoethanol; 50°C, 30 min) using an anti- $\beta$ -actin antibody (Sigma) at a dilution of 1:1,000. Particle incorporation of EBOV-GPs was detected using a GP1-specific rabbit serum at a 1:1,000 dilution. To show that equal amounts of pseudotypes and replication-competent virus were used, a separate membrane with the same samples was incubated with an antibody against VSV-M (matrix protein, raised in mice [KeraFast];

1:1,000). Bound antibodies were detected using horseradish peroxidase (HRP)-linked anti-mouse or anti-rabbit secondary antibodies (Dianova) at a dilution of 1:10,000. Signals of bound secondary antibodies were detected using an in-house-made enhanced chemiluminescence (ECL) solution (0.1 M Tris-HCl, pH 8.6, 250  $\mu$ g/ml luminol [Sigma], 1 mg/ml *para*-hydroxycoumaric acid [Sigma], 0.3% H<sub>2</sub>O<sub>2</sub>) and visualized using a ChemoCam imaging system along with the ChemoStar Professional software (Intas).

**Virus-like particle release assay.** Release of HIV-Gag or EBOV-VP40-based virus-like particles (VLPs) was analyzed as described before (10) to assess the importance of the GXXXA motif for EBOV-GP-dependent tetherin antagonism. In brief, 293T cells were seeded in 48-well plates and cotransfected following calcium-phosphate precipitation with plasmid encoding HIV-1 p55-Gag or EBOV-VP40, human tetherin, and a tetherin antagonist or empty plasmid as control. At 48 h posttransfection, supernatants were collected and clarified from cell debris, and VLPs were pelleted by centrifugation through a 20% sucrose cushion. Concentrated VLPs were resuspended in 20  $\mu$ l of 2 $\times$  SDS buffer. In parallel, cells were lysed with 50  $\mu$ l of 2 $\times$  SDS lysis buffer. Both whole-cell lysates (WCL) and VLPs were boiled at 95°C for 30 min. Presence of HIV-Gag in lysates and VLPs was analyzed by immunoblotting according to the same protocol as described in the previous paragraph ("Immunoblotting"). Gag protein was detected using a 1:100 diluted supernatant of hybridoma cells secreting a mouse anti-Gag antibody (183-H12-5C) (41), while EBOV-VP40 was detected using undiluted supernatants of 9E10 cells, a hybridoma cell line that secretes anti-Myc antibody (42). Finally, antibody binding was detected employing an HRP-linked anti-mouse secondary antibody (Dianova) at a dilution of 1:10,000.

**Statistical analyses.** To assess statistical significance, unpaired and paired Student *t* tests were conducted for comparison of two data groups, while one-way analysis of variance (ANOVA) with Bonferroni posttest analysis was conducted for comparison of multiple data groups. All statistical analyses were done employing the GraphPad Prism software (GraphPad Software).

## ACKNOWLEDGMENTS

The following reagents were obtained through the NIH AIDS Reagent Program, Division of AIDS, NIAID, NIH: the HeLa cell line from Richard Axel and anti-HIV-1 p24 hybridoma (183-H12-5C) from Bruce Chesebro. We thank G. Herrler for BHK-21(G43) cells and M. Müller and C. Drosten for EpoNi/22.1 cells.

The work of Michael Schindler (SCHI1073/4-1) and Stefan Pöhlmann (PO 716/8-1) was funded by Deutsche Forschungsgemeinschaft (DFG). Mariana González-Hernández was funded by the Deutscher Akademischer Austauschdienst (DAAD) country-related cooperation program with Mexico (CONACYT, Consejo Nacional de Ciencia y Tecnología) (stipend).

## REFERENCES

1. Chow J, Franz KM, Kagan JC. 2015. PRRs are watching you: Localization of innate sensing and signaling regulators. *Virology* 479–480:104–109. <https://doi.org/10.1016/j.virol.2015.02.051>.
2. Schneider WM, Chevillotte MD, Rice CM. 2014. Interferon-stimulated genes: a complex web of host defenses. *Annu Rev Immunol* 32:513–545. <https://doi.org/10.1146/annurev-immunol-032713-120231>.
3. Schoggins JW, Wilson SJ, Panis M, Murphy MY, Jones CT, Bieniasz P, Rice CM. 2011. A diverse range of gene products are effectors of the type I interferon antiviral response. *Nature* 472:481–485. <https://doi.org/10.1038/nature09907>.
4. Thompson MR, Kaminski JJ, Kurt-Jones EA, Fitzgerald KA. 2011. Pattern recognition receptors and the innate immune response to viral infection. *Viruses* 3:920–940. <https://doi.org/10.3390/v3060920>.
5. Erikson E, Adam T, Schmidt S, Lehmann-Koch J, Over B, Goffinet C, Harter C, Bekeredjian-Ding I, Sertel S, Lasitschka F, Keppler OT. 2011. In vivo expression profile of the antiviral restriction factor and tumor-targeting antigen CD317/BST-2/HM1.24/tetherin in humans. *Proc Natl Acad Sci U S A* 108:13688–13693. <https://doi.org/10.1073/pnas.1101684108>.
6. Neil SJ, Zang T, Bieniasz PD. 2008. Tetherin inhibits retrovirus release and is antagonized by HIV-1 Vpu. *Nature* 451:425–430. <https://doi.org/10.1038/nature06553>.
7. Perez-Caballero D, Zang T, Ebrahimi A, McNatt MW, Gregory DA, Johnson MC, Bieniasz PD. 2009. Tetherin inhibits HIV-1 release by directly tethering virions to cells. *Cell* 139:499–511. <https://doi.org/10.1016/j.cell.2009.08.039>.
8. Neil SJ. 2013. The antiviral activities of tetherin. *Curr Top Microbiol Immunol* 371:67–104. [https://doi.org/10.1007/978-3-642-37765-5\\_3](https://doi.org/10.1007/978-3-642-37765-5_3).
9. Messaoudi I, Amarasinghe GK, Basler CF. 2015. Filovirus pathogenesis and immune evasion: insights from Ebola virus and Marburg virus. *Nat Rev Microbiol* 13:663–676. <https://doi.org/10.1038/nrmicro3524>.
10. Brinkmann C, Nehlmeier I, Walendy-Gnirrs K, Nehls J, Gonzalez HM, Hoffmann M, Qiu X, Takada A, Schindler M, Pöhlmann S. 2016. The tetherin antagonism of the Ebola virus glycoprotein requires an intact receptor-binding domain and can be blocked by GP1-specific antibodies. *J Virol* 90:11075–11086. <https://doi.org/10.1128/JVI.01563-16>.
11. Kaletsky RL, Francia JR, Agrawal-Gamse C, Bates P. 2009. Tetherin-mediated restriction of filovirus budding is antagonized by the Ebola glycoprotein. *Proc Natl Acad Sci U S A* 106:2886–2891. <https://doi.org/10.1073/pnas.0811014106>.
12. Kühl A, Banning C, Marzi A, Votteler J, Steffen I, Bertram S, Glowacka I, Konrad A, Sturz M, Guo JT, Schubert U, Feldmann H, Behrens G, Schindler M, Pöhlmann S. 2011. The Ebola virus glycoprotein and HIV-1 Vpu employ different strategies to counteract the antiviral factor tetherin. *J Infect Dis* 204(Suppl 3):S850–S860. <https://doi.org/10.1093/infdis/jir378>.
13. Lopez LA, Yang SJ, Hauser H, Exline CM, Haworth KG, Oldenburg J, Cannon PM. 2010. Ebola virus glycoprotein counteracts BST-2/tetherin restriction in a sequence-independent manner that does not require tetherin surface removal. *J Virol* 84:7243–7255. <https://doi.org/10.1128/JVI.02636-09>.
14. Lopez LA, Yang SJ, Exline CM, Rengarajan S, Haworth KG, Cannon PM. 2012. Anti-tetherin activities of HIV-1 Vpu and Ebola virus glycoprotein do not involve removal of tetherin from lipid rafts. *J Virol* 86:5467–5480. <https://doi.org/10.1128/JVI.06280-11>.
15. Vande Burgt NH, Kaletsky RL, Bates P. 2015. Requirements within the Ebola viral glycoprotein for tetherin antagonism. *Viruses* 7:5587–5602. <https://doi.org/10.3390/v7102888>.
16. Gnirß K, Fiedler M, Kramer-Kuhl A, Bolduan S, Mittler E, Becker S, Schindler M, Pöhlmann S. 2014. Analysis of determinants in filovirus glycoproteins required for tetherin antagonism. *Viruses* 6:1654–1671. <https://doi.org/10.3390/v6041654>.
17. Hacke M, Bjorkholm P, Hellwig A, Himmels P, Ruiz de Almodovar C, Brugger B, Wieland F, Ernst AM. 2015. Inhibition of Ebola virus

- glycoprotein-mediated cytotoxicity by targeting its transmembrane domain and cholesterol. *Nat Commun* 6:7688. <https://doi.org/10.1038/ncomms8688>.
18. Bavari S, Bosio CM, Wiegand E, Ruthel G, Will AB, Geisbert TW, Hevey M, Schmaljohn C, Schmaljohn A, Aman MJ. 2002. Lipid raft microdomains: a gateway for compartmentalized trafficking of Ebola and Marburg viruses. *J Exp Med* 195:593–602. <https://doi.org/10.1084/jem.20011500>.
  19. Noda T, Sagara H, Suzuki E, Takada A, Kida H, Kawaoka Y. 2002. Ebola virus VP40 drives the formation of virus-like filamentous particles along with GP. *J Virol* 76:4855–4865. <https://doi.org/10.1128/JVI.76.10.4855-4865.2002>.
  20. Kühl A, Hoffmann M, Muller MA, Munster VJ, Gnirss K, Kiene M, Tsegaye TS, Behrens G, Herrler G, Feldmann H, Drosten C, Pöhlmann S. 2011. Comparative analysis of Ebola virus glycoprotein interactions with human and bat cells. *J Infect Dis* 204(Suppl 3):S840–S849. <https://doi.org/10.1093/infdis/jir306>.
  21. Licata JM, Johnson RF, Han Z, Harty RN. 2004. Contribution of Ebola virus glycoprotein, nucleoprotein, and VP24 to budding of VP40 virus-like particles. *J Virol* 78:7344–7351. <https://doi.org/10.1128/JVI.78.14.7344-7351.2004>.
  22. Simmons G, Wool-Lewis RJ, Baribaud F, Netter RC, Bates P. 2002. Ebola virus glycoproteins induce global surface protein down-modulation and loss of cell adherence. *J Virol* 76:2518–2528. <https://doi.org/10.1128/jvi.76.5.2518-2528.2002>.
  23. Yang ZY, Duckers HJ, Sullivan NJ, Sanchez A, Nabel EG, Nabel GJ. 2000. Identification of the Ebola virus glycoprotein as the main viral determinant of vascular cell cytotoxicity and injury. *Nat Med* 6:886–889. <https://doi.org/10.1038/78645>.
  24. Garbutt M, Liebscher R, Wahl-Jensen V, Jones S, Moller P, Wagner R, Volchkov V, Klenk HD, Feldmann H, Stroher U. 2004. Properties of replication-competent vesicular stomatitis virus vectors expressing glycoproteins of filoviruses and arenaviruses. *J Virol* 78:5458–5465. <https://doi.org/10.1128/JVI.78.10.5458-5465.2004>.
  25. Takada A, Feldmann H, Stroehrer U, Bray M, Watanabe S, Ito H, McGregor M, Kawaoka Y. 2003. Identification of protective epitopes on ebola virus glycoprotein at the single amino acid level by using recombinant vesicular stomatitis viruses. *J Virol* 77:1069–1074. <https://doi.org/10.1128/JVI.77.2.1069-1074.2003>.
  26. Liberatore RA, Mastrocola EJ, Powell C, Bieniasz PD. 2017. Tetherin inhibits cell-free virus dissemination and retards murine leukemia virus pathogenesis. *J Virol* 91:e02286-16. <https://doi.org/10.1128/JVI.02286-16>.
  27. Weidner JM, Jiang D, Pan XB, Chang J, Block TM, Guo JT. 2010. Interferon-induced cell membrane proteins, IFITM3 and tetherin, inhibit vesicular stomatitis virus infection via distinct mechanisms. *J Virol* 84:12646–12657. <https://doi.org/10.1128/JVI.01328-10>.
  28. Radoshitzky SR, Dong L, Chi X, Clester JC, Retterer C, Spurgers K, Kuhn JH, Sandwick S, Ruthel G, Kota K, Boltz D, Warren T, Kranzusch PJ, Whelan SP, Bavari S. 2010. Infectious Lassa virus, but not filoviruses, is restricted by BST-2/tetherin. *J Virol* 84:10569–10580. <https://doi.org/10.1128/JVI.00103-10>.
  29. Maddon PJ, Dalgleish AG, McDougal JS, Clapham PR, Weiss RA, Axel R. 1986. The T4 gene encodes the AIDS virus receptor and is expressed in the immune system and the brain. *Cell* 47:333–348. [https://doi.org/10.1016/0092-8674\(86\)90590-8](https://doi.org/10.1016/0092-8674(86)90590-8).
  30. Hanika A, Larisch B, Steinmann E, Schwegmann-Wessels C, Herrler G, Zimmer G. 2005. Use of influenza C virus glycoprotein HEF for generation of vesicular stomatitis virus pseudotypes. *J Gen Virol* 86:1455–1465. <https://doi.org/10.1099/vir.0.80788-0>.
  31. Hoffmann M, Crone L, Dietzel E, Pajio J, Gonzalez-Hernandez M, Nehlmeier I, Kalinke U, Becker S, Pöhlmann S. 2017. A polymorphism within the internal fusion loop of the Ebola virus glycoprotein modulates host cell entry. *J Virol* 91:e00177-17. <https://doi.org/10.1128/JVI.00177-17>.
  32. Sauter D, Schindler M, Specht A, Landford WN, Munch J, Kim KA, Votteler J, Schubert U, Bibollet-Ruche F, Keele BF, Takehisa J, Ogando Y, Ochsenbauer C, Kappes JC, Ayouba A, Peeters M, Learn GH, Shaw G, Sharp PM, Bieniasz P, Hahn BH, Hatzioannou T, Kirchhoff F. 2009. Tetherin-driven adaptation of Vpu and Nef function and the evolution of pandemic and nonpandemic HIV-1 strains. *Cell Host Microbe* 6:409–421. <https://doi.org/10.1016/j.chom.2009.10.004>.
  33. Martin-Serrano J, Zang T, Bieniasz PD. 2001. HIV-1 and Ebola virus encode small peptide motifs that recruit Tsg101 to sites of particle assembly to facilitate egress. *Nat Med* 7:1313–1319. <https://doi.org/10.1038/nm1201-1313>.
  34. Schnell MJ, Buonocore L, Whitt MA, Rose JK. 1996. The minimal conserved transcription stop-start signal promotes stable expression of a foreign gene in vesicular stomatitis virus. *J Virol* 70:2318–2323.
  35. Hoffmann M, Gonzalez HM, Berger E, Marzi A, Pöhlmann S. 2016. The glycoproteins of all filovirus species use the same host factors for entry into bat and human cells but entry efficiency is species dependent. *PLoS One* 11:e0149651. <https://doi.org/10.1371/journal.pone.0149651>.
  36. Berger Rentsch M, Zimmer G. 2011. A vesicular stomatitis virus replicon-based bioassay for the rapid and sensitive determination of multi-species type I interferon. *PLoS One* 6:e25858. <https://doi.org/10.1371/journal.pone.0025858>.
  37. Lawson ND, Stillman EA, Whitt MA, Rose JK. 1995. Recombinant vesicular stomatitis viruses from DNA. *Proc Natl Acad Sci U S A* 92:4477–4481.
  38. Sutter G, Ohlmann M, Erfle V. 1995. Non-replicating vaccinia vector efficiently expresses bacteriophage T7 RNA polymerase. *FEBS Lett* 371:9–12. [https://doi.org/10.1016/0014-5793\(95\)00843-X](https://doi.org/10.1016/0014-5793(95)00843-X).
  39. Dietzel E, Kolesnikova L, Sawatsky B, Heiner A, Weis M, Kobinger GP, Becker S, M von V, Maisner A. 2015. Nipah virus matrix protein influences fusogenicity and is essential for particle infectivity and stability. *J Virol* 90:2514–2522. <https://doi.org/10.1128/JVI.02920-15>.
  40. Krähling V, Becker D, Rohde C, Eickmann M, Eroglu Y, Herwig A, Kerber R, Kowalski K, Vergara-Alert J, Becker S. 2016. Development of an antibody capture ELISA using inactivated Ebola Zaire Makona virus. *Med Microbiol Immunol* 205:173–183. <https://doi.org/10.1007/s00430-015-0438-6>.
  41. Chesebro B, Wehrly K, Nishio J, Perryman S. 1992. Macrophage-tropic human immunodeficiency virus isolates from different patients exhibit unusual V3 envelope sequence homogeneity in comparison with T-cell-tropic isolates: definition of critical amino acids involved in cell tropism. *J Virol* 66:6547–6554.
  42. Evan GI, Lewis GK, Ramsay G, Bishop JM. 1985. Isolation of monoclonal antibodies specific for human c-myc proto-oncogene product. *Mol Cell Biol* 5:3610–3616. <https://doi.org/10.1128/MCB.5.12.3610>.